

MaxNet: Faster Flow Control Convergence

Bartek P. Wydrowski^{*,†}, Lachlan L. H. Andrew^{*}, Iven M. Y. Mareels^{*}.

^{*}The ARC Special Research Centre for Ultra-Broadband Information Networks.
Department of Electrical and Electronic Engineering, The University of Melbourne,
Australia. {b.wydrowski,l.andrew,i.mareels}@ee.mu.oz.au

[†]NetLab, Department of Computer Science, California Institute of Technology

Abstract. MaxNet is a distributed congestion control architecture in which only the most severely bottlenecked link on the end-to-end path controls the source rate. This paper shows that the small-signal convergence speed of MaxNet is higher than that of conventional architectures, such as the current Internet or REM. It also shows that MaxNet decouples the control, so that each pole position depends only on parameters of one bottleneck link and of the sources controlled by that bottleneck, enabling optimal pole placement.

1 Introduction

Network flow control aims to control source rates so that link capacities are utilised. Internet-like networks, where links and sources can only have local information, must use fully distributed control.

Models of Internet-like networks control the source rate by a scalar feedback congestion signal which aggregates the congestion prices of links on the end-to-end connection. The signals, such as loss or delay, used by current flow control algorithms such as TCP, are implicitly summed over all links by the network. We refer to these networks as SumNets. In [1], we introduced MaxNet, where the congestion prices are aggregated by taking the maximum link price along the connection path, rather than the sum. In [1], we showed that MaxNet results in Max-Min fairness for sources with homogeneous demand functions.

Sufficient conditions for the stability of MaxNet are known [2], but its transient dynamics are yet to be studied. The convergence time of network flow control impacts on the Quality of Service of the network. A slow response results in long traffic transients which are responsible for packet delay, delay-jitter, under-utilisation and buffer-overflow. Reducing the duration and overshoot of transients improves these performance measures and makes smaller buffer sizes possible.

This paper compares the convergence times of MaxNet and SumNet, using a common framework given in Section 2. The first part of the investigation involves a local analysis for which we develop small-signal linearized models in Sections 3 and 4. Using these models, Section 6 finds the position of poles which determine the convergence time of MaxNet. Section 7 compares the convergence time of MaxNet with a lower bound of the performance of SumNet, and shows that a

faster pole placement is possible with MaxNet than with SumNet. This makes it possible for MaxNet to achieve better QoS performance. In the second part of this paper, Section 8 investigates the global performance by simulating the full non-linear system, and relates the local analysis to these simulation results.

2 Control Architecture

The following is a brief overview of the MaxNet and SumNet control algorithms. For a fuller description, see [1, 3]. The behaviour of source i is governed by an explicit demand function, $D_i(\cdot)$, such that its transmit rate is

$$x_i = D_i(q_i) \quad (1)$$

for a congestion signal q_i . In both MaxNet and SumNet, the congestion signal, q_i , summarises the prices, p_l , of all links, l , on the end-to-end path, L_i , of source i . In MaxNet the congestion signal is the maximum of all link prices,

$$q_i = \max\{p_l : l \in L_i\}. \quad (2a)$$

In contrast, SumNet uses the sum

$$\hat{q}_i = \sum_{l \in L_i} p_l. \quad (2b)$$

(Throughout this paper, variables with a hat pertain to SumNet, and the corresponding variables without a hat pertain to MaxNet.)

The Active Queue Management (AQM) algorithm in a router sets the price of an outgoing link according to the well studied integrator process [3]:

$$p_l(t+1) = p_l(t) + (y_l(t) - c_l)\varphi_l, \quad (3)$$

where $y_l(t) = \sum_{i:l \in L_i} x_i(t)$ is the aggregate traffic for link l at time t , φ_l is the control gain and c_l is the target capacity of link l which is related to its physical capacity, C_l by the target utilisation, $0 < \mu_l < 1$, such that $c_l = \mu_l C_l$.

3 MaxNet Control System Model

This section describes the MaxNet model from [2] which will be used in subsequent sections to investigate convergence time. This model makes a number of simplifications of the network. The first is to use a fluid-flow approximation of the packet based information flow. The second simplification is that the global non-linear system is linearized about its equilibrium point. MaxNet contains two sources of non-linearity. The first is the Max operation itself and the second is the non-linear demand function, D . These will be linearised separately.

Using these simplifications, the network is represented as a multi-variable control system, shown in Figure 1. Note that Figure 1, for illustration only, shows

a large-signal source, and small-signal links and network. The interconnection of sources with links is piecewise linear, due to the Max operation. It is described in the Laplace domain by forward and backward routing matrices. The matrices specify the interconnection and the delay incurred in signal flow from source to link and vice versa. The forward routing matrix is

$$[\bar{R}_f(s)]_{l,i} = \begin{cases} e^{-\tau_{i,l}^f s} & \text{if source } i \text{ uses link } l \\ 0 & \text{otherwise,} \end{cases} \quad (4)$$

where $\tau_{i,l}^f s$ is the forward delay between source i and link l . Note that the bar notation in $\bar{R}_f(s)$ indicates it has a row for every link in the network. We later reduce this to a matrix representing only bottleneck links, without the bar.

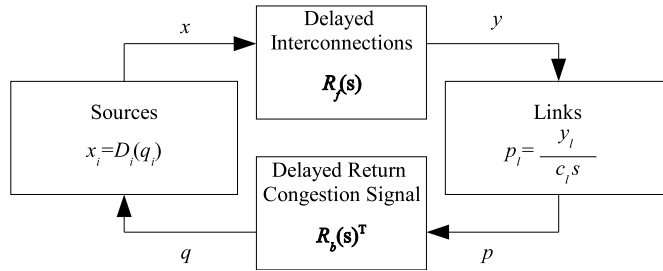


Fig. 1. Flow Control Structure.

Let n_i be the bottleneck link that controls source i (the link on L_i with the maximum price). Then the backward routing matrix depends on n , as

$$[\bar{R}_b(s; n)]_{l,i} = \begin{cases} e^{-\tau_{i,l}^b s} & \text{if } n_i = l \\ 0 & \text{otherwise.} \end{cases} \quad (5)$$

Note that the round-trip time of source i 's connection is $\tau_i = \tau_{i,l}^f + \tau_{i,l}^b$. Let L be the number of links in the network. Without loss of generality, order the link prices such that

$$p_1 \geq p_2 \geq \dots \geq p_L. \quad (6)$$

The backward routing matrix remains static over a period where the variations in link prices do not change the ordering of link prices (6). The overall multi-variable feedback loop in the configuration of Figure 1 is

$$\bar{y}(s) = \bar{R}_f(s)x(s) \quad (7)$$

$$q(s) = \bar{R}_b(s; n)^T \bar{p}(s). \quad (8)$$

We can construct a small signal model as in [3]. Consider small perturbations around equilibrium, $x = x_0 + \delta x$, $\bar{y} = \bar{y}_0 + \delta \bar{y}$, $\bar{p} = \bar{p}_0 + \delta \bar{p}$, $q = q_0 + \delta q$, where

subscript 0 denotes a steady state value and prefix δ denotes a perturbation. Note that the bar notation still denotes variables that contain non-bottleneck links and $\delta\bar{p}_l$ is only non-zero for bottleneck links. Note also that when all link prices are distinct, the vector of bottlenecks, n , is unchanged by a sufficiently small perturbation. In this case, the small signal model does not explicitly involve n . This is the first linearisation. Form the vectors $\delta p(s)$, $\delta y(s)$ and the matrices R_f , R_b by eliminating the elements (or rows) corresponding to non-bottleneck links. This gives the reduced small signal model

$$\delta y(s) = R_f(s)\delta x(s) \quad (9)$$

$$\delta q(s) = R_b(s)^T \delta p(s). \quad (10)$$

To achieve stable control for networks of arbitrary dimensions, it is sufficient that the gains that sources and links introduce be as follows [2]. The second linearisation replaces the demand function of a source by a small-signal gain, κ_i , between a perturbation in δq_i and the resulting perturbation in δx_i , given by

$$\kappa_i = D'_i(q_i). \quad (11)$$

For robust stability, it is sufficient that this gain be scaled such that

$$\kappa_i = \frac{\alpha_i x_{0i}}{\tau_i}. \quad (12)$$

Here, $\alpha_i \in (0, 1)$ reflects the source's need for capacity, and the factor τ_i provides robustness to delay. To make stability robust to the number of sources, a gain x_{0i}/c_l is introduced in the closed-loop, with the x_{0i} component put into the source and the $1/c_l$ component in the link as $\varphi_l = 1/c_l$.

Note that (11) implicitly assumes a static demand function. As discussed in [3], the requirement (12) determines the shape of the static demand function. However, recent work in [4] provides dynamic source algorithms which allow arbitrary demand functions, whilst preserving the control gain required for robust stability. They separate the high-frequency gain AC from the DC gain.

In the Laplace domain, the integrator AQM of (3) with the required gain between the coupling of δp_l and δy_l is

$$\delta p_l = \frac{1}{c_l s} \delta y_l. \quad (13)$$

The open-loop transfer function for the small signal MaxNet model is

$$H(s) = \frac{1}{s} R_f(s) \mathcal{K} R_b(s)^T \mathcal{C}, \quad (14)$$

where

$$\mathcal{K} = \text{diag}(\kappa_i), \quad \mathcal{C} = \text{diag}\left(\frac{1}{c_l}\right). \quad (15)$$

4 SumNet Control System Model

This section describes the model from [3] for a SumNet network, by highlighting the difference from the MaxNet model. Recall that the hat symbol identifies SumNet variables which have a related variable in MaxNet.

The SumNet forward routing matrix is the same as that of MaxNet, $\hat{\bar{R}}_f = \bar{R}_f$. The backward routing matrix, which describes the flow of congestion information from each link back to sources, is independent of the current transmission rates:

$$[\hat{\bar{R}}_b(s)]_{l,i} = \begin{cases} e^{-\tau_{i,l}^b s} & \text{if source } i \text{ uses link } l \\ 0 & \text{otherwise.} \end{cases} \quad (16)$$

Thus (8) becomes

$$q(s) = \hat{\bar{R}}_b(s)^T \bar{p}(s). \quad (17)$$

The small signal variables also take on the hat notation: $\hat{x} = \hat{x}_0 + \delta\hat{x}$, $\hat{y} = \hat{y}_0 + \delta\hat{y}$, $\hat{p} = \hat{p}_0 + \delta\hat{p}$, $\hat{q} = \hat{q}_0 + \delta\hat{q}$.

For SumNet, the routing matrices can again be reduced to contain only bottleneck links. These reduced matrices are applicable so long as the bottlenecks remain the same throughout the perturbations. The reduced small-signal model has the same form as (9), (10), in the variables $\hat{R}_f = R_f$, \hat{R}_b , $\delta\hat{p}(s)$ and $\delta\hat{q}(s)$.

To achieve stable control for networks of arbitrary dimensions, the gains that sources and links introduce need to satisfy the bounds detailed in [3]. For SumNet, a source i requires a gain $\hat{\kappa}_i$ of

$$\hat{\kappa}_i = \frac{\hat{\alpha}_i \hat{x}_{0i}}{M_i \tau_i}, \quad (18)$$

where M_i is the number of controlling bottleneck links on the end-to-end path, and $\hat{\alpha}_i \in (0, 1)$ is again an adjustable parameter.

To maintain stability, SumNet must either estimate and communicate M_i to each source [3], or use a slow, conservative control policy. MaxNet has $M_i = 1$, eliminating these drawbacks.

The complete SumNet open loop small signal transfer function has the same form as (14), (15).

5 Root Loci

Despite their non-linear nature, the small signal convergence behaviour of MaxNet and SumNet can be characterised by the positions of the dominant poles of their linearisation. The MaxNet case is described; SumNet is analogous.

The closed-loop transfer function is

$$T(s) = G(s)(Is + G(s))^{-1}, \quad (19)$$

where $G(s) = sH(s)$. The poles of $T(s)$ are values of s satisfying either of the equivalent equations

$$\det(I + H(s)) = 0 \quad \text{or} \quad \text{eig}(H(s)) = -1. \quad (20)$$

For non-zero poles, corresponding conditions are

$$\det(Is + G(s)) = 0 \quad \text{or} \quad \text{eig}(G(s)) = -s. \quad (21)$$

The root loci of MaxNet and SumNet have many similarities, but some important differences. The open loop transfer function of each has L poles at zero. In MaxNet, these correspond directly to the sources controlled by the L links. In SumNet, there is intrinsic coupling between the links, and it is not helpful to think of poles as belonging to particular links.

For very small, but positive, loop gain, the poles at the origin move left on the real line. Meanwhile, L infinite sets of poles appear with real part $-\infty$, and with imaginary parts uniformly spaced [5]. These poles move right in the complex plane as the loop gains are increased. Importantly, L of these poles move along the real axis. For MaxNet, it is once again possible to associate each pole with a specific link, while for SumNet, the poles can only be associated with eigenvalues of a less structured matrix.

The point at which the rightmost of the poles coming from infinity meets the leftmost of the poles coming from zero is called a breakpoint. At this point, the two poles become a complex-conjugate pair, and start moving at right angles to the real axis, before going right again to eventually cross the imaginary axis and cause instability. As the gains increase further, subsequent pairs of real poles will meet at their respective break points, and also eventually become unstable. Under MaxNet, the pairs of poles which meet at break points always belong to the same link.

The value of the maximum real pole is minimised at the break point, when two real solutions of (20) coincide. At that point, s_l^* , not only are the left and right hand sides equal, but their derivatives are also equal [6].

6 MaxNet Convergence Time

This section will derive bounds on the fastest possible convergence time of MaxNet; that is, the most negative value the real part of the dominant pole as the feedback gain is varied. These results hold for MaxNet networks with arbitrary topology, delay, number of sources and capacity.

Lemma 1. *For sufficiently small gain, each link, l , introduces a pair of real poles. The minimum value achieved (by increasing the gain) of the maximum of these poles is the break point, s_l^* , which lies between $-1/t_{\max_l}$ and $-1/t_{\min_l}$, where t_{\max_l} and t_{\min_l} are the maximum and minimum round trip times (RTTs) of all of the sources being controlled by link l .*

Proof. Since $G(s)$ is lower triangular under MaxNet, the eigenvalues are simply the diagonal elements, each of which corresponds to a particular link. Thus (21) decouples, and we get one equation per link. From (14), poles associated with link l satisfy

$$-s = \sum_{k \in m_l} \frac{a_k e^{-\tau_k s}}{c_l}, \quad (22)$$

where

$$a_i = \frac{\alpha_i x_{0i}}{\tau_i}. \quad (23)$$

Each of these equations clearly has a real solution for sufficiently small a_i , establishing the first part of the lemma.

Differentiating (22) to find the break point, s_l^* , yields the condition

$$1 = \sum_{k \in m_l} \frac{a_i \tau_i e^{-\tau_i s_l^*}}{c_l} = \sum_{k \in m_l} b_i, \quad (24)$$

where

$$b_i = \frac{a_i \tau_i e^{-\tau_i s_l^*}}{c_l}. \quad (25)$$

Substituting (25) into (22) gives

$$-s_l^* = \sum_{k \in m_l} \frac{b_i}{\tau_i}. \quad (26)$$

Since $1 = \sum_{k \in m_l} b_i$, then (26) is a weighted sum of $1/\tau_i$. A weighted sum is between the maximum and minimum elements in the sum, giving

$$-\frac{1}{\tau_{\min_l}} \leq s_l^* \leq -\frac{1}{\tau_{\max_l}}. \quad (27)$$

Proposition 1. *At the break point, s_l^* is the dominant pole due to link l .*

Proof. Except for the pole at the origin, all poles of (19) start with infinitely negative real part for low loop gain. Thus it suffices to show that, as the loop gain is increased, no complex pole crosses the line $\text{Re}(s) = s_l^*$ before the real pole starting at $-\infty$ does.

Substituting $s = -\sigma + j\omega$ into (22) yields the implicit equation for pole positions at link l

$$\sum_{k \in m_l} a_k e^{\sigma \tau_k} (\cos(\omega \tau_k) - j \sin(\omega \tau_k)) = \sigma c_l - j\omega c_l. \quad (28)$$

Taking the real part of (28) gives

$$\sum_{k \in m_l} a_k e^{\sigma \tau_k} \cos(\omega \tau_k) = \sigma c_l. \quad (29)$$

Consider a line on the complex plane where $\text{Re}(s) = \sigma$. If we fix the operating point for parameters x_{0k} and τ_k , then by (28), a is element-wise minimized when $\omega = 0$. Since complex poles begin at negative infinity for $a = 0$, and for the minimum a_{\min} that satisfies (28) there is only a real pole on the line $\text{Re}(s) = \sigma$, it follows that the real pole is the first to cross this line as the gain is increased. Complex poles, with $\omega \neq 0$, that cross this line have an element-wise higher a , and are therefore to the left of the real pole when the gain is a_{\min} . Thus the real pole at the break point will be the dominant pole for that link, since no complex poles have crossed to its right.

Remark 1. A key conclusion from this analysis is that because the links are independent, it is possible to adjust the control gains such that all links are simultaneously at their break points. That implies that the fastest operation of MaxNet is governed by poles satisfying (27).

7 Bound on SumNet Convergence Time

This section will show that, at least for the specific case analysed, MaxNet has a faster transient response than SumNet.

Due to the complexity of the SumNet analysis, we will consider a two link SumNet network only, where all sources have a common round trip time, τ , and only one source traverses both links. The assumption of a common round trip time is expected to favour SumNet by reducing the coupling between link. Thus we have no reason to believe that any other SumNet will be able to achieve a faster transient response than the equivalent MaxNet. It is sufficient to consider only the real pole, even though there may be complex poles which are slower, since this gives a lower bound for the transient response time.

The SumNet system can be described by a 2×2 open-loop transfer function matrix, \hat{H} . Expanding the SumNet form of (14) gives the elements of \hat{H} as

$$\hat{H}_{ij}(s) = \frac{1}{sc_j} \sum_{k \in U_i \cap U_j} e^{-(\tau_{k_i}^F + \tau_{k_j}^B)s} \hat{a}_k, \quad (30)$$

where U_i is the set of sources that uses link i and

$$\hat{a}_k = \frac{\hat{\alpha}_k x_{0k}}{M_k \tau_k}. \quad (31)$$

The following lemmas are proved in the appendix.

Lemma 2. *For a two link SumNet, where only one source traverses both links, and all sources have the same RTT τ , the unique break point is at $-1/\tau$.*

Lemma 3. *Unless $\hat{\alpha}_k = 0$ for all k , $\hat{G}(s)$ for a two link SumNet does not have a repeated eigenvalue for real s .*

Together, these two lemmas imply that there must be a pole to the right of $-1/\tau$. Therefore SumNet must have a slower transient response than MaxNet.

8 Numerical Results

In this section, the full non-linear SumNet and MaxNet networks are simulated to compare their transient response speeds. The results are evidence that the small signal linearized properties proven analytically in the previous sections are relevant to the practical non-linear system.

The system simulated in this section is intended to reflect a physically realisable system. Whilst it may be possible to devise a control strategy where each

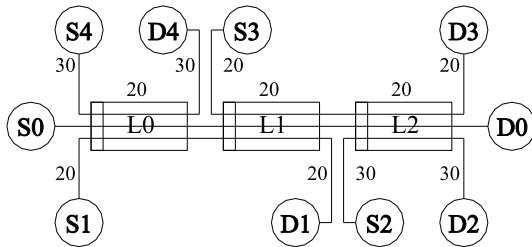


Fig. 2. Network Simulated.

source measures network properties and tunes its own gains (equation (18) for SumNet or (12) for MaxNet) to optimize transient speed, an online algorithm to achieve this is not trivial. In this paper we consider a practical strategy where all sources use the same demand function. We simulate sources with the same static demand function

$$x_i(t) = x_{\max} e^{-\rho q_i(t)} \quad (32)$$

where ρ is a network wide parameter and x_{\max} is the maximum transmission rate. A similar demand function was introduced in [3], and was shown to be able to satisfy the gain requirements (12). For MaxNet, the parameter ρ relates to the small-signal source gain (12) such that

$$\rho = \frac{\alpha_i x_{0i}}{\tau_i} \quad (33)$$

and for SumNet the equivalent relationship is with (18)

$$\rho = \frac{\hat{\alpha}_i x_{0i}}{M_i \tau_i} \quad (34)$$

Note that ρ may be tuned to improve transient performance. This strategy will in general not result in the fastest possible transient response for MaxNet or SumNet, as the poles are not necessarily placed at their closet position to the break-points. Nevertheless it allows us to demonstrate some important properties.

A small network of 5 sources and 3 links, shown in Figure 2, is simulated using both SumNet and MaxNet congestion signaling. Sources $S_0 \dots S_4$ transmit to destinations $D_0 \dots D_4$ respectively.

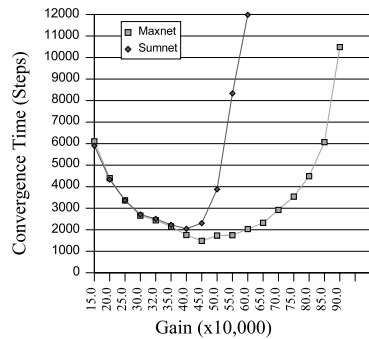
We model traffic by a fluid flow approximation, that is, the source transmission rate and congestion price are continuous. At each time step in this discrete time simulation, the flow rate values and price feedback move one unit along in the forward and backward delay paths between sources and links. Acknowledgements are assumed to traverse the same links in the reverse direction, and consume negligible bandwidth. The numbers near each line in Figure 2 represent delays, in simulation time step units. Note that every source has a RTT of 160 units, and for all sources x_{\max} is set to 15. The MaxNet or SumNet link control

law (3) is at the head of the link, represented by the rectangle inside each link in Figure 2.

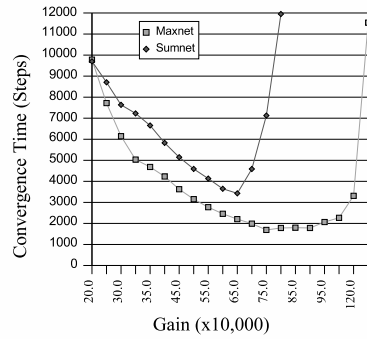
In the simulation scenarios, we assume that the best-effort congestion controlled traffic is receiving only a portion of the link’s physical capacity. This represents the situation of having higher-priority constant-bit-rate (CBR) traffic occupying some capacity. We simulate two scenarios with different proportions of CBR traffic and different link capacities.

In Scenario 1, the physical link capacities are $c_0 = 5$, $c_1 = 3$ and $c_2 = 5$. To generate a transient, we assume that initially the capacities available to best-effort traffic are 5, 3 and 2 at links L_0 , L_1 and L_2 respectively. A transient occurs when the CBR traffic source using L_2 stops and the available capacities become 5, 3 and 5. Throughout the whole experiment the link gains are, as stipulated in [3], $1/c_l$ such that $\varphi_0 = 1/5$, $\varphi_1 = 1/3$ and $\varphi_2 = 1/5$.

Scenario 2 is the same as scenario 1 except that the physical link capacity of link 1 is $c_1 = 12$, and correspondingly $\varphi_1 = 1/12$. The available capacities again start at 5, 3 and 2, and link 2’s available capacity increases to 5.



(a) Simulation scenario 1



(b) Simulation scenario 2

Fig. 3. SumNet and MaxNet Convergence Time.

The transient response metric used is the settle time, which is the time from the change of capacity to when the last source is within $\pm 1\%$ of its final value. The settle time is measured in simulation time steps. Figures 3(a) and 3(b) show this convergence time for both SumNet and MaxNet for gains $\rho = 0.0015$ to $\rho = 0.009$ for scenario 1, and $\rho = 0.002$ to $\rho = 0.012$ for scenario 2.

9 Conclusion and Acknowledgement

This paper has shown that MaxNet flow control has favourable convergence properties compared with traditional SumNet flow control. For small perturbations from the operating point, MaxNet permits a pole placement that has a faster transient response than that possible with SumNet. Numerical results for the complete nonlinear system confirm the conclusions drawn from the analysis of the linear model.

This work was funded by the Australian Research Council.

References

1. Wydrowski, B., Zukerman, M.: MaxNet: A congestion control architecture for maxmin fairness. *IEEE Commun. Lett.* **6** (2002) 512–514
2. Wydrowski, B., Andrew, L.L.H., Zukerman, M.: MaxNet: A congestion control architecture for scalable networks. *IEEE Commun. Lett.* **7** (2003) 511–513
3. Paganini, F., Doyle, J.C., Low, S.H.: Scalable laws for stable network congestion control. In: *Proc. IEEE Conf. Decision Contr. (CDC)*, Orlando, FL (2001) 185–90
4. Paganini, F., Wang, Z., Low, S., Doyle, J.: A new TCP/AQM for stable operation in fast networks. In: *Proc. IEEE Infocom*, San Francisco, CA (2003) 96–105
5. Marshall, J.E., Górecki, H., Walton, K., Korytowski, A.: *Time-Delay Systems: Stability and Performance Criteria with Applications*. Ellis Horwood, New York, NY (1992)
6. Ogata, K.: *Modern Control Engineering*. Prentice-Hall, Englewood Cliffs, NJ (1970)

Appendix

The proof of Lemma 2 is as follows.

Proof. This proof will again use the fact that, at the point at which a pair of real poles meet and become complex conjugates, the derivative of $X = \det(I + \hat{H}(s))$ with respect to s is zero. It also uses the fact that values of s for which $dX/ds = 0$ but $X \neq 0$ are not breakpoints.

Since the round trip time of each route is equal, $\tau_{ki}^F + \tau_{ki}^B = \tau$ for all k , (30) implies

$$\hat{H}_{ii}(s) = \frac{1}{sc_i} \sum_{k \in U_i} e^{-\tau s} \hat{a}_k = \frac{e^{-\tau s}}{s} R_i, \quad (35)$$

for $i = 1, 2$, where $R_i = \sum_{k \in U_i} \hat{a}_k / c_i$.

The fact that only one source traverses both links implies that, for $i \neq j$, the sum in (30) contains a single term. Without loss of generality, let that source be source 1. Then

$$\begin{aligned} \hat{H}_{12}(s) \hat{H}_{21}(s) &= \frac{\hat{a}_1^2}{s^2 c_1 c_2} e^{-(\tau_{11}^F + \tau_{12}^B + \tau_{12}^F + \tau_{11}^B)s} \\ &= \frac{e^{-2\tau s}}{s^2} R_3, \end{aligned} \quad (36)$$

where $R_3 = \hat{a}_1^2 / (c_1 c_2)$.

From (20), the 2×2 SumNet poles are at $X = 0$, where

$$X = \hat{H}_{11}(s)\hat{H}_{22}(s) - \hat{H}_{12}(s)\hat{H}_{21}(s) + \hat{H}_{11}(s) + \hat{H}_{22}(s) + 1.$$

Substituting (35) and (36) into this gives

$$X = \frac{e^{-2\tau s}}{s^2}(R_1 R_2 - R_3) + \frac{e^{-\tau s}}{s}(R_1 + R_2) + 1. \quad (37)$$

Differentiating (37) to find the break point gives

$$\begin{aligned} \frac{dX}{ds} &= (\tau s + 1) \left(\frac{2e^{-2\tau s}}{s^3}(R_1 R_2 - R_3) - \frac{e^{-\tau s}}{s^2}(R_1 + R_2) \right) \\ &= (\tau s + 1) A \frac{2e^{-\tau s}(R_1 R_2 - R_3) - s(R_1 + R_2)}{s^3}, \end{aligned} \quad (38)$$

where

$$A \equiv \frac{e^{-\tau s}}{s}.$$

This derivative, (38), is zero when $s = -1/\tau$. The root locus occupies the entire negative real axis, and thus $s^* = -1/\tau$ corresponds to an actual breakpoint. It remains to show that there are no other breakpoints.

Assume, with a view to obtaining a contradiction, that there is another breakpoint, s' . At s' , the final factor of (38) must be zero. That implies

$$\frac{e^{-\tau s}}{s} = \frac{R_1 + R_2}{2(R_1 R_2 - R_3)}. \quad (39)$$

Substituting (39) into (37) gives

$$X = \frac{3(R_1 + R_2)^2}{4(R_1 R_2 - R_3)} + 1.$$

But the left hand side is positive, since R_3 is one of the terms in the positive-term sum $R_1 R_2$, and so $X \neq 0$. Thus s' is not a pole, and cannot be a breakpoint. This establishes the result.

The proof of Lemma 3 is as follows.

Proof. The eigenvalues of $\hat{G}(s)$ are

$$\hat{G}_{11}(s) + \hat{G}_{22}(s) \pm \sqrt{(\hat{G}_{11}(s) - \hat{G}_{22}(s))^2 + 4\hat{G}_{21}(s)\hat{G}_{12}(s)}. \quad (40)$$

Equating the two solutions to (40) gives the condition for poles being coincident as

$$0 = (\hat{G}_{11}(s) - \hat{G}_{22}(s))^2 + 4\hat{G}_{21}(s)\hat{G}_{12}(s). \quad (41)$$

When s is real, $\hat{G}_{ij}(s)$ is also real. A real solution to (41) is only possible when $\hat{G}_{21}(s)\hat{G}_{12}(s) \leq 0$. For SumNet, $\hat{G}_{21}(s)\hat{G}_{12}(s) > 0$ for real s , unless $\hat{a}_k = 0$ for all k . Thus (41) cannot be satisfied.